View metadata, citation and similar papers at core.ac.uk

brought to you by CORE

provided by The University of North Carolina at Greensboro

METABOLIC INFLUENCES OF FIBER SIZE IN AEROBIC AND ANAEROBIC MUSCLES OF THE BLUE CRAB, *Callinectes sapidus*.

Lisa K. Johnson

A Thesis Submitted to the
University of North Carolina at Wilmington in Partial Fulfillment
Of the Requirements for the Degree of
Master of Science

Department of Biological Sciences

University of North Carolina at Wilmington

2004

Approved by

Advisory Committee

_____ _____

_____
Chair

Accepted by

_____
Dean, Graduate School

TABLE OF CONTENTS

ABSTRACT iii

ACKNOWLEDGMENTS iv

LIST OF FIGURES vi

LIST OF TABLES vii

INTRODUCTION 1

MATERIALS AND METHODS 5

Animals 5

Transmission Electron Microscopy 6

Citrate Synthase Activity 8

In vivo Fatigue 8

L-Lactate Assays 10

Statistical Analysis 10

RESULTS 11

Subdivision Diameters and Mitochondrial Fractional Area 11

Citrate Synthase Activity 12

Lactate Production and Removal 12

DISCUSSION 14

REFERENCES 37

ABSTRACT

Diameters of some white muscle fibers in the adult blue crab, *Callinectes sapidus*, exceed 500 μm whereas juvenile white fibers are <100 μm. It is hypothesized that aerobically dependent processes, such as recovery from exercise, will be significantly impeded by size in these large white fibers. In addition, dark aerobic fibers of adults, which do rely on aerobic contraction, grow as large as the white fibers. These large aerobic fibers are subdivided, thus decreasing the effective diameter of the fiber and enabling aerobic contraction. The two goals of this study were: (1) to characterize the development of subdivisions in the dark muscle fibers and (2) to monitor post-contractile metabolism as a function of fiber size. Dark muscle fibers from crabs ranging from <0.1 g to >200 g were examined with transmission electron microscopy to determine the density of mitochondria and subdivision diameters. Mitochondrial fractional areas were consistently 25% of the total subdivision area and subdivision sizes remained constant throughout development, with an average diameter of 36.5 ± 2.7 μm. Citrate synthase (CS) activities in dark muscle were higher and scaled with a steeper negative slope (b=-0.19) than activities in white muscle (b=-0.09). In addition, the time course of [lactate] was monitored during recovery from anaerobic, burst exercise in white and dark muscle and hemolymph. Burst escape responses were elicited in crabs ranging from <1 g to >200 g and [lactate] measured. There were no differences among size classes with respect to lactate accumulation as a result of exercise, however, in white fibers from large crabs, lactate continued to increase after exercise, and lactate removal from tissues required a longer period of time relative to small and medium crabs. Differences in lactate removal among size classes were less pronounced in dark fibers. These data suggest that in addition to normal metabolic scaling, aerobic metabolic processes are limited to SA:V and intracellular diffusion constraints in large white muscle fibers.

ACKNOWLEDGEMENTS

First, I would like to express my appreciation and gratitude to numerous individuals who donated their time and energy to help collect crabs for this project: Kristin Andrews (with Marinequest, Beth Rhine's class from Myrtle Grove Middle School, and Summer By The Sea Camp), Al Nyack (with Boy Scout Troops), Patrick Kennedy, Bailey Lee, Jesse Gore, Kristin Hardy, Fay Belshe, Brandy Hutchins, Britt Edelman, Soma Sarkar, Martyn Knowles, and David Fickle. Also, thank you to East Coast Seafood (corner of 14th and Dawson Sts.) and Howard's Seafood (501 Castle St.) for having adult crabs available year-round.

An extra special thank you goes out to Mark Gay, without whom this project would not have been possible. Thank you for having a great sense of humor, having lots of patience, and for teaching me how to use the TEM, the microtome, Adobe Photoshop and Image Pro Plus, and helping me trouble-shoot aspect of my project along the way.

Thank you to my fellow lab-mates (past and present) for making lab work fun: (grads.) Soma Sarkar, Melissa Ernst, Al Nyack, Kristin Hardy, (undergrads.) Bailey Lee, Jesse Gore, Martyn Knowles, Brandy Hutchins, Tyler Balak, and Stacy Ballard. Thank you, again, to Britt for helping to feed and maintain the crab tanks.

And thank you to my parents, John and Kristi Johnson, for immense patience, understanding, and continued loving support. Thank you to Pat Kennedy for keeping me company and providing lots of moral support during my time here at UNCW.

Thank you to my thesis committee members, Drs. Pabst and Roer, and my departmental reader, Dr. Dillaman, for providing helpful and insightful comments along the way on aspects of this project as well as on this thesis.

Thank you to Dr. Blum for lots of patience and help with SAS code and statistical analysis of this data.

And lastly, but not least, thank you to my advisor Dr. Steve Kinsey for being a great teacher and mentor, and for giving me a piece of this cell size story to work on for my masters project. Being a graduate student wouldn't have been nearly as much fun with a different project.

LIST OF FIGURES

Figure Page

1. Arginine kinase (AK) mediates ATP-equivalent flux in crustacean muscle 22

2. Dark levator muscle fiber subdivision development 24

3. Mean mitochondrial fractional areas (open bars, left axis) and mean fiber subdivision diameters (filled bars, right axis) of the dark levator aerobic muscle fibers with respect to animal size class 26

4. Mass-specific scaling of citrate synthase (CS) activity per gram of white levator (open circles, data from Boyle *et al*. 2003) and dark levator muscle (filled circles).....28

5. Lactate (mM) concentrations at rest, 1 min after exercise, and 60 min after exercise in (A) white levator and (B) dark levator muscles 30

6. Time course of lactate concentration changes in (A) white and (B) dark levator muscles, and (C) hemolymph following fatiguing exercise 32

7. The area under the lactate concentration recovery curve for each tissue vs. size class.....34

LIST OF TABLES

Table Page

1. Size classes of crabs used in this study based on body mass and white levator fiber diameter data from Boyle et al. (2003) and dark fiber subdivision data derived from TEM analysis 36

INTRODUCTION

Cells typically fall within a size range of 10-100 μm along the shortest axis (e.g. Russell et al., 2000). Dimensions exceeding this range are thought to compromise aerobic metabolism, which relies upon oxygen flux across cell membranes (e.g. Kim et al., 1998), as well as ATP-equivalent flux from mitochondria to sites of ATP demand (Mainwood and Rakusan, 1982). However, some muscle fibers from crustaceans do not adhere to the usual constraints on cellular dimensions, and in the adult blue crab, *Callinectes sapidus*, fiber diameters from the white locomotor muscles that power swimming often exceed 500 μm (Tse et al., 1983; Boyle et al., 2003). In contrast, white fibers from juvenile *C. sapidus* are <100 μm in diameter, meaning that during development these fibers cross and exceed the usual limit on cell dimensions while preserving burst-contractile function (Boyle et al., 2003).

An interesting feature of these white muscle fibers is that the distribution of mitochondria varies as a function of fiber size. In juveniles, mitochondria are uniformly distributed throughout the fibers and the population is equally divided between subsarcolemmal and intermyofibrillar fractions. However, in white fibers from adults, mitochondria are exclusively subsarcolemmal. Thus, in large fibers there is a cylinder of oxidative potential around the periphery of the cell whereas the inner core of the fiber has virtually no aerobic capacity (Boyle et al., 2003). This developmental redistribution of mitochondria dramatically increases intracellular diffusion distances between mitochondria in large fibers, more so than would be expected from increases in fiber diameter alone. Since contraction in these fibers is anaerobically-powered and does not rely upon oxygen flux across the cell membrane or intracellular diffusion of ATP-equivalents from mitochondria to sites of ATP demand, large cell size should not impact this process. However, the small surface area to volume ratios (SA:V) and intracellular diffusion limitations

associated with large fiber size would be expected to affect aerobic metabolism. This is consistent with observations that post-contractile recovery in muscle from adult *C. sapidus* is a very slow process (Milligan et al., 1989; Henry et al., 1994).

Burst contraction in crustacean muscles is similar to that in vertebrates, where intracellular phosphagen and glycogen stores are depleted and lactic acid accumulates (England and Baldwin, 1983; Booth and McMahon, 1985; Head and Baldwin, 1986; Milligan et al., 1989; Morris and Adamczewska, 2002). In crustaceans, there is an initial reliance on the hydrolysis of the phosphagen, arginine phosphate (AP), after which anaerobic glycogenolysis is recruited to generate additional ATP. Glycogenolytically-powered contractions are slower than those powered by phosphagen hydrolysis (England and Baldwin, 1983; Head and Baldwin, 1986; Baldwin et al., 1999; Boyle et al., 2003), and lactate only accumulates during an extended series of anaerobic contractions. Since *C. sapidus* demonstrates resistance to fatigue induced by elevated lactate levels/acidic pH, it is likely that extended high-force contractions are a normal part of the animal's behavior in the environment (Booth and McMahon, 1992).

In contrast to anaerobic contraction, the recovery from sustained exercise in crustaceans is quite different from the vertebrate paradigm. An early phase of recovery is a restoration of AP pools. This step of recovery is largely powered by anaerobic glycogenolysis (England and Baldwin, 1983; Head and Baldwin, 1986), which contrasts with the exclusively aerobic resynthesis of the vertebrate phosphagen, creatine phosphate (PCr) (Kushmerick, 1983; Meyer, 1988; Curtin et al., 1997). Thus, in crustaceans most glycogen depletion and lactate accumulation occurs after contraction (England and Baldwin, 1983; Head and Baldwin, 1986; Kamp, 1989; Henry et al., 1994; Morris and Adamczewska, 2002; Boyle et al., 2003). The reasons for this post-contractile lactate accumulation in crustacean muscle are not known.

However, it may be a mechanism for accelerating certain phases of the recovery process to facilitate additional high-force contractions, since exclusive reliance on aerobic metabolism would be expected to result in an extremely slow recovery in very large fibers (Boyle et al., 2003). Therefore, in crustaceans anaerobic metabolism would be expected to contribute to post-contractile recovery more in large fibers than in small fibers.

Despite reliance upon anaerobic metabolism to power specific recovery processes, complete recovery ultimately must depend on aerobic pathways. Since mitochondria are located around the periphery of the fiber in large cells, the aerobic phase of recovery is dependent upon diffusive flux of ATP-equivalents from the mitochondria to points of utilization in the fiber core (Boyle et al., 2003). The phosphoryl transfer from ATP to arginine forming AP is catalyzed by arginine kinase (AK), which functions near equilibrium in crustacean muscle (Ellington, 2001; Holt and Kinsey, 2002). Since the ATP-equivalent diffusive flux is carried almost exclusively by AP, aerobic processes are dependent on the rate of AP diffusive flux (Meyer et al., 1984; Ellington and Kinsey, 1998; Kinsey and Moerland, 2002), which is strongly hindered by structural barriers in crustacean muscle (Kinsey et al. 1999; Kinsey and Moerland, 2002) (Fig. 1). The scope of diffusion limitation can be appreciated by examining the time required for intracellular metabolite diffusion in muscle. In juvenile blue crabs, diffusion of AP across a muscle fiber takes place in several seconds, whereas in adults the time required for diffusion across a fiber can exceed 20 minutes (Kinsey and Moerland, 2002). It is therefore expected that diffusion limitations will increasingly constrain the rate of aerobic post-exercise recovery as animals become larger.

In addition to white locomotor muscles, *C. sapidus* also have smaller bundles of mitochondria-rich, dark fibers that power aerobic swimming (Tse et al., 1983), and these fibers

must also maintain contractile function over a 3,000-fold increase in body mass during post-metamorphic development. There are two general mechanisms by which an organism can increase its muscle mass during post-embryonic growth (reviewed in Rowlerson and Veggetti, 2001). New muscle fibers can develop through hyperplasia as seen in cephalopods (e.g. Pecl and Moltschaniwskyj, 1997) or existing fibers can increase in diameter through hypertrophy as seen in fishes (e.g. Weatherly and Gill, 1985) and crustaceans (Bittner and Traut, 1978). Whereas the large developmental increase in body mass in *C. sapidus* causes white locomotor muscle fibers to become giant (Boyle et al., 2003), the aerobic function of the dark muscle fibers necessitates that they remain small. *C. sapidus* appears to have resolved the conflicting demands for hypertrophic development and aerobic contraction by subdividing the dark fibers into smaller functional units (Tse et al., 1983). While the development of white locomotor fibers has been previously described by Boyle et al. (2003), the ontogenetic development of the aerobic fibers has not been addressed. For instance, it is unclear whether a constant number of aerobic subdivisions are present in fibers from all size classes, including the smallest fibers from juvenile animals where diffusion would not be expected to limit aerobic processes, or whether subdivisions form throughout development and function to maintain a constant, small size of each aerobic functional unit. If a relatively constant number of subdivisions occurs throughout development, then muscle from juvenile animals would have extremely small subdivisions, which may be disadvantageous because tissue volume that could be devoted to myofibrillar contractile elements would be limited (Rome and Lindstedt, 1998). A constant subdivision size obviates this potential problem, and may indicate the maximal fiber/subdivision size that can support aerobic contractile function.

The objectives of the present study were: (1) to characterize the post-metamorphic developmental pattern of subdivision formation in the dark levator swimming muscle, which constitutes a giant fiber system that has undergone selection for aerobic function, and (2) to assess the reliance on anaerobic metabolism of white and dark fibers during post-contractile recovery. I investigated mitochondrial content, the scaling of aerobic enzyme activity, and subdivision formation in fibers of the dark levator muscle during post-metamorphic growth in *C. sapidus*. Lactate levels following fatiguing exercise were monitored in white and dark levator muscle tissues as well as in hemolymph. I hypothesized that: (1) dark fibers would grow hypertrophically, but subdivisions would form throughout development to maintain a constant, small effective diameter; (2) post-contractile lactate accumulation would be greater and removal would be slower in white fibers from large crabs than in small crabs; and (3) post-contractile lactate accumulation would not occur in dark levator muscle due to the absence of intracellular diffusive limitations in the small, subdivided fibers.

MATERIALS AND METHODS

Animals

Juvenile crabs were collected from April to November 2003 by sweep netting in the basin of the Cape Fear River, NC (salinity range 0-15 ppt), and adult crabs were purchased from April to December 2003 from local seafood vendors (Wilmington, NC). All crabs were transported to UNCW where they were placed in aerated, full-strength (35 ppt, 1000 mOsmol/L) seawater no more than two hours after acquisition and acclimated for at least one week before the experiments. Crabs were maintained on a 12:12 h light:dark cycle and fed bait shrimp (Cape Point Bait Co.) or Crab & Lobster Bites® (HBH Pet Products) three times per week. Only

intermolt crabs were used as determined by the rigidity of the carapace, the presence of the membranous layer of the carapace, and the absence of soft cuticle forming beneath the old exoskeleton (Roer and Dillaman, 1984).

Transmission Electron Microscopy

To characterize the developmental pattern of the dark levator muscle, the diameters of the fiber subdivisions and their corresponding mitochondrial fractional areas were measured with transmission electron microscopy (TEM). Twelve crabs ranging in body mass from <0.1 g to >250 g were divided into four size classes referred to as very small, small, medium, and large (Table 1). Crabs were sacrificed by removing the dorsal carapace. The dark levator muscles (Cochran, 1935, White and Spirito, 1973, Tse *et al.* 1983) were exposed by removal of the reproductive and digestive organs, gills, and portions of the endoskeleton, and mechanically isolated from surrounding tissue. Resting length of the muscle was measured from its origin on the median plate to the insertion at the heavy tendon while the fifth periopod (swimming leg) was positioned as far antero-dorsally as possible. A small bundle of dark levator fibers were teased apart with a glass probe, tied off with 6-0 surgical silk, and then excised from the animal. Due to the heterogeneity of the fiber composition in dark levator muscle, care was taken to isolate only the core of the tissue, which is comprised of aerobic fibers (Tse et al. 1983). The fiber bundle was placed at resting length in a primary fixative consisting of 1% glutaraldehyde and 4% paraformaldehyde in 0.063 M Sörenson's phosphate buffer, pH 7.38 (Egginton and Sidell, 1984; Preshnell and Schriebman, 1997). The osmolarity of the fixative and all corresponding buffer rinses were adjusted by the addition of 10% sucrose and a trace amount of $CaCl_2$ to prevent a change in cell volume. Tissues were held in primary fixative for a minimum of twenty-four hours at room temperature then rinsed for fifteen minutes in Sörenson's

phosphate buffer. This process was followed by a secondary fixation in 1% osmium tetraoxide, in Sörenson's phosphate buffer. Samples were then dehydrated with an ascending series (50%, 70%, 95%, 100%, 100%) of ethanol and embedded in Spurr's epoxy resin (Spurr, 1969; Electron Microscopy Sciences). Samples were sectioned at 90 nm with a diamond knife on a Reichert Ultracut E and collected using a systematic random sampling method (Howard and Reed, 1998) to ensure complete representation of the mitochondrial distribution throughout the muscle. Five sections were collected from a random starting point, and then a distance of 500 nm was skipped before collecting another five sections. This process was repeated until 5 μm of tissue was sectioned. Five sections were mounted on each Formvar-coated (0.25% Formvar in ethylene dichloride) high-transmission copper grid and were stained with 2% uranyl acetate in 50% ethyl alcohol and with Reynolds' lead citrate (Reynolds, 1963). Sections were examined with a Philips CM-12 TEM operated at 60kV. One section per grid was randomly chosen and a montage of photographs (3,600x) was generated from a 100 μm^2 region of dark fibers. Montage photographs were obtained from 5 sections per animal to yield 60 total micrographs used for mitochondrial fractional area and fiber subdivision diameter analysis, this was to account for intra vs. inter individual variation. Negatives were developed and then digitized using a Microtek Scanmaker 4 negative scanner.

Adobe Photoshop (version 7.0) was used to process images. Micrographs were montaged and the mitochondria as well as the fiber subdivisions were individually outlined. Image Pro Plus (version 4.1.0.9) software was used to calculate fiber subdivision diameters and areas of the outlined fiber subdivisions. In addition, Image Pro Plus was used to calculate fractional areas of the outlined mitochondria. For each animal, fractional areas were calculated by dividing the

mitochondrial area summed over all 5 micrographs for that animal by the total subdivision area summed over all 5 micrographs for each animal.

Citrate Synthase Activity

Citrate synthase (CS) activity measurements were used as a measure of aerobic capacity, and were examined as a function of animal size in dark levator muscle. The scaling of white levator CS activity with body mass was measured previously by Boyle et al. (2003). Dark levator muscle tissues were excised from 23 crabs ranging in body mass from <1 g to >200 g (Table 1). Tissues were extracted in 5-20 volumes of extraction buffer (50 mM Tris, 1 mM EDTA, 2 mM $MgCl_2$, 2 mM dithiothreitol, pH 7.6) and sonicated on ice at 6 W using 4 bursts of 5 s each. Samples were centrifuged at 16,000 x *g* for 20 min, and the supernatants were stored at -80°C until further analysis.

Citrate synthase activities were spectrophotometrically assayed at 25°C using the methods of Walsh and Henry (1990). The supernatant was combined with 1 mM 5,5-dithio-bis [2-nitrobenzioc acid], 0.3 mM acetylcoenzyme A, and water in a 0.5 mL cuvette for a baseline absorbance reading at 412 nm on an Ultrospec 4000 spectrophotometer (Pharmacia) until the absorbance stabilized. The reaction was initiated by the addition of 0.5 mM oxaloacetate and the enzyme activity ($\mu mol \cdot min^{-1} \cdot g^{-1}$) was calculated using the slope of the absorbance change immediately following the addition of oxaloacetate.

In vivo Fatigue

To determine the ontogenetic reliance on anaerobic metabolism in white and dark levator fibers during post-contractile recovery, burst contractile activity comparable to that during an escape response was elicited by stimulating the thoracic ring ganglia (Boyle et al. 2003). Only the three largest size classes of crab (Table 1) were used for these experiments due to the

difficulty of obtaining sufficient quantities of tissue for metabolite extractions in the very small animals. The size classes used were defined based on the relationship between animal weight and white levator fiber size described by Boyle et al. (2003). In white muscle, the mean diameters (μm) of the fibers were 133.3 ± 1.9, 226.0 ± 4.2, 462.4 ± 22.0 for small, medium, and large animals, respectively (Boyle et al., 2003).

Crabs were removed from aquaria and suspended in the air with a clamp such that the swimming leg motion was unrestricted. Wire electrodes were placed in two small holes drilled into the mesobranchial region of the dorsal carapace, and a Grass Instruments SD9 physiological stimulator (Astro-Med, Inc.) was used to elicit contractile responses (80 Hz, 200 ms duration at 70 V). A single 200 ms pulse would induce a series of burst swimming contractions that typically lasted from 2-20 s. Stimulations were repeated once every minute until the animal was fatigued, determined by minimal response to stimulation. Following exercise, crabs were immediately placed in aerated aquaria, provided with food, and allowed to recover for one of eight time periods (1, 10, 60, 90, 120, 240, 360, 480 min following exercise). Due to the expected longer recovery period for large crabs (Henry et al., 1994, Boyle et al., 2003), this group was allowed to recover for 720 min following exercise and recovery at 90 min was not examined. At least 5 animals per size class were not exercised. These animals were weighed and measured then allowed to rest overnight before the tissue collection. A minimum of 4 crabs were used per time point, and the mean N value for all time points was 6.8.

Immediately before sacrifice, hemolymph was collected with a syringe from the arthrodial membrane at the base of the swimming leg and frozen in liquid nitrogen. The crabs were sacrificed by removing the dorsal carapace. White and dark levator muscle tissues were

quickly dissected as previously described, samples were excised, freeze-clamped in liquid nitrogen, and stored at -80°C until further analysis.

L-Lactate Assays

Frozen tissue samples (0.05-0.2 g) were homogenized in 9-29 volumes of chilled 7% perchloric acid using a PowerGen (Fisher) homogenizer, sonicated on ice at 6 W using 4 bursts of 5 s each, then centrifuged at 4°C at 16,000 x *g* for 20 min. The supernatants were neutralized using 3 M KCO_3^- in 50 mM PIPES and centrifuged at 4ºC at 16,000 x *g* for 20 min. The resulting supernatants were stored at -80°C.

The concentration of L-lactate in white levator, dark levator, and hemolymph was spectrophotometrically assayed following the procedures of Lowry and Passonneau (1972). A buffer containing 300 mM hydrazine hydrate, 12 mM EDTA, and 4 mM NAD^+ at pH 9.0 was mixed with the supernatant in a 0.5 mL cuvette and read at 340 nm on an Ultraspec 4000 (Pharmacia) to obtain a baseline absorbance value. The reaction was initiated by the addition of 18.5 units of L-lactate dehydrogenase, and the change in absorbance was measured. The concentration in the sample was calculated assuming that 1 g of white and dark levator muscle tissue has 0.75 mL of intracellular water (Milligan et al., 1989).

Statistical Analysis

Levene's test was used to test for heteroscedascity. One-way analysis of variance (ANOVA) was used to test for the main effects of animal size class on fiber subdivision diameter, mitochondrial fractional area, and citrate synthase activity. Where significant size effects were detected, Tukey's HSD test was used to make pairwise comparisons among the means from animal size classes. Two-way ANOVA was used to analyze the post-contractile lactate concentrations for effects of size class and recovery time, as well as the interaction

between animal size class and recovery time for each tissue type. To compare lactate recovery in the dark and white fibers, a three-way ANOVA was used to test for a significant interaction of animal size class, recovery time, and muscle type. All statistical tests were analyzed with JMP software version 7.0.2 (SAS institute) or SAS software version 8.02. Results were considered significant if $p<0.05$. The linear regression of CS activity data (Fig. 4) and the area under the [lactate] recovery curve (Fig. 7) were calculated using Sigma Plot software version 8.02 (SPSS Inc.). Data are represented as mean ± S.E.M. throughout.

RESULTS

Subdivision Diameters and Mitochondrial Fractional Area

The dark levator aerobic fibers were identified from surrounding white and intermediate fibers based on dense concentrations of mitochondria and the presence of smaller fiber subunits. Individual aerobic fibers in the dark levator were identified by the presence of a surrounding membrane and relatively large gaps separating fibers. The subdivisions found within the fiber were identified by the presence of a surrounding membrane and a very minimal gap of space separating the subdivisions. Hemocytes were frequently observed in regions surrounding the whole fiber as well as between subdivisions. This implies that the subdivisions are highly perfused with hemolymph, which is consistent with being an aerobic muscle.

Neither the diameters of the dark levator muscle aerobic fiber subdivisions ($F=0.25$, $df=3$, $p=0.86$) nor the mitochondrial fractional areas of the subdivisions ($F=0.065$, $df=3$, $p=0.98$) changed during development (Fig. 2; Fig. 3). The mean diameter of the subdivisions across all size classes was 35.6 ± 2.7 μm, which is well within the range of cellular dimensions typical of aerobic fibers from other animals. Although the mean diameter of the dark levator fiber

subdivisions did not change, the total number of subdivisions did increase throughout development. For example, the fibers from the very small size class have no subdivisions while subdivisions do exist in the fibers of the small, medium, and large size classes (Fig. 2). The mitochondria were distributed almost exclusively around the periphery of these aerobic fiber subdivisions, and they represented between 20-30% of the total area of each subdivision (Fig. 3).

Citrate Synthase Activity

Citrate synthase (CS) activity in dark levator muscle scaled negatively with increasing body mass (Fig. 4A). CS activity levels were higher in dark levator than in white levator, as expected from the difference in function of these muscles. A line was fitted to the data according to the scaling relationship CS activity = $a \cdot M^b$, where M is animal mass, a is a constant, and b is the scaling exponent (Schmidt-Nielsen, 1984). When grouped by animal size class, there was a significant effect of size on CS activity ($F=14.6$, $df=2$, $p<0.001$), and mean CS activity in dark muscle from large animal size class was < ½ of the activity in muscle from the small size class.

Lactate Production and Removal

The lactate concentration values were $\log_{10}$ transformed to achieve homogeneous variance. One-way ANOVA was used to test for a significant effect of animal size class on each of the tissue types for [lactate] at rest, immediately following exercise, and 60 min post-exercise. Resting lactate concentrations were not significantly different among animal size classes for white levator ($F=2.0$, $df=2$, $p=0.16$; Fig. 5A), dark levator ($F=3.31$, $df=2$, $p=0.054$) (Fig. 5B), or hemolymph ($F=1.02$, $df=2$, $p=0.37$). All size classes of crab responded similarly to stimulations, although smaller crabs tended to have contractile bursts that were of a higher frequency but shorter duration than large crabs. However, immediately following exercise there were no differences among size classes in the amount of lactate produced during exercise in

white ($F=1.02$, $df=2$, $p=0.38$) or dark levator muscle ($F=0.602$, $df=2$, $p=0.56$) (Fig. 5), suggesting that muscle from all size classes of animals were doing the same amount of mass-specific anaerobic work during exercise. During recovery from exercise, however, there were large differences in [lactate] among animal size classes. This pattern was particularly apparent at 60 min post-exercise where [lactate] reached the highest levels observed in large white fibers, which led to a significant effect of animal size class ($F=14.3$, $df=2$, $p=<0.001$) (Fig. 5A). There was also a significant effect of animal size class in the dark levator at 60 min post-exercise ($F=6.9$, $df=2$, $p=0.01$), although the differences were not as great as were seen in the white levator.

A complete time course of lactate production and removal is presented in Figure 6. Lactate levels began to decline immediately following exercise in both muscle tissues from small and medium crabs, while lactate remained elevated in both muscle tissues from large crabs, and the subsequent time course of lactate removal in all tissues from large crabs required greater than 480 min. Unexpectedly, dark levator muscle from large crabs appeared to require more time for lactate clearance than small and medium crabs (Fig. 6B), although the differences between the size classes in lactate removal from dark levator muscle appeared to be considerably less than the differences between size classes in the white levator (Fig. 6A). The hemolymph time course mirrored that of the two muscle tissues, but peak lactate concentrations tended to lag slightly behind those for the muscles. Two-way ANOVA was run separately for each tissue, and all three tissues had significant interactions between size and recovery time (white levator: $F=4.6$, $df=11$, $p<0.001$; dark levator: $F=4.5$, $df=11$, $p<0.001$; hemolymph: $F=3.5$, $df=11$, $p<0.001$). To analyze potential differences between the dark and light levator muscle, a three-way ANOVA was run to test for a significant interaction of animal size class, muscle type, and recovery time.

Despite the apparent differences between the two muscle types, there was not a significant three-way interaction ($F=1.3$, $df=15$, $p=0.18$).

To further illustrate differences between size and tissue on dark and white muscle lactate concentrations during recovery, the area under the lactate removal curve was calculated for each tissue from each size class using the trapezoidal rule of integration with Sigma Plot (version 8.02) (Fig. 7). There appeared to be very large differences among size classes using this approach, particularly in the white fibers.

DISCUSSION

The first objective of this study was to characterize the post-metamorphic development of the dark levator muscle aerobic fiber subdivisions. Several authors have described the presence of fiber subdivisions within adult crustacean muscle fibers (Rosenbluth, 1969; Jahromi and Atwood, 1971). Histochemical staining of the dark levator fibers in adult *C. sapidus* by Tse et al. (1983) showed that aerobic fibers are highly subdivided into smaller functional units with diameters much less than 100 μm, while the overall fiber diameter is similar to that in white levator muscle (several hundred microns). In the present study, low magnification microraphs showed that in all size classes the diameters of the aerobic fibers were consistent with those of white levator fibers described by Boyle et al. (2003). Subdivision formation in these dark aerobic muscle fibers was expected to occur in one of two ways: (1) the subdivisions are innate features of the dark aerobic fibers and are present in the smallest post-metamorphic crabs, and subdivision diameter increases throughout development, or (2) the muscle fibers are not originally subdivided, but become so during development. Evidence from this study supports the latter hypothesis. The dark fibers from the smallest animals examined (<0.1 g) had little or no

subdivision, but they became increasingly subdivided throughout post-metamorphic development (Fig. 2).

Striated skeletal muscle is a post-mitotic and highly differentiated tissue that has little capability of increasing by simple division of its component fibers. In fishes, hyperplasia occurs until a certain point in development, after which muscle mass is increased by hypertrophy of existing fibers (reviewed in Weatherly and Gill, 1987), although there are exceptions to this generalization. For example, fiber division appears to occur in adult specimens of the fishes, *Notothenia coriiceps* and *Patagonotothen longipes* (Johnston et al., 2003). Several fibers, in the absence of myoblasts, divided into daughter fibers that led to a small (1-3%) increase in fiber number and muscle mass. Fiber splitting was also noted in the mullet, *Mugil cephalus* (Carpené and Veggetti, 1981) and in the European eel, *Anguilla anguilla* (Willemse and Lieuwma-Noordanaus, 1984). In contrast, squid muscle growth occurs via hyperplasia and is the principle means of increasing muscle mass during post-embryonic development (e.g. Pecl and Moltschaniwskyj, 1997; Preuss et al., 1997). Blue crab dark levator muscle is perhaps unique in that it appears to grow hypertrophically, but because of the large developmental increase in body mass, the fibers that power swimming become exceptionally large. However, aerobic swimming is maintained by fiber subdivisions and intra-fiber perfusion with hemolymph. The result of this fiber subdivision is the developmental maintenance of a constant size of each *metabolic* functional unit while there is a simultaneous increase in the size of each *contractile* functional unit.

These results also imply that there is a maximal size at which the aerobic locomotor muscle fibers of blue crabs are able to contract aerobically. Above this size, low SA:V and long intracellular diffusive distances may begin to constrain the rate of oxygen and ATP fluxes such

that they are insufficient to keep pace with the high demands of contraction. While fiber subdivisions may solve problems of SA:V and diffusion, they are accompanied by spatial constraints, and the fact that subdivisions are not seen in fibers less than 60 μm may indicate that small fiber/subdivision size leads to diminished space available for myofilaments, which would lead to a reduction in force production (Rome and Lindstedt, 1998).

The high CS activities and mitochondrial densities in aerobic muscle fibers were roughly five-fold higher than that in white levator fibers (Boyle et al., 2003) and are consistent with observations that adult *C. sapidus* have exceptional aerobic, long-distance swimming capabilities (Judy and Dudley, 1970). Although the negative allometric scaling of CS activity (Fig. 4) was similar to the findings in white levator muscle (Boyle et al., 2003), these data contrast with that for mitochondrial fractional area in the dark aerobic fiber subdivisions, which did not scale negatively with body mass (Fig. 3). This result was unexpected and it may indicate that the mitochondria from the smaller animals are more densely packed with aerobic enzymes. Alternatively, the discrepancy between the mitochondrial fractional area and CS activity data could be due to differences in the method of data collection. CS activity data was referenced to the wet weight of the whole muscle, whereas the TEM analyses of mitochondria were based on cross-sectional areas within a fiber subdivision excluding extracellular and extra-subdivision spaces. There may be systematic differences in the scaling of, for example, intra- and extracellular water content of the muscles that would be accounted for in the activity measurements but not in the TEM analyses.

The second objective of this study was to examine some of the metabolic implications of hypertrophic growth in crustacean muscle fibers with the assumption that increasing fiber size in white muscle and the accompanying mitochondrial shift towards the periphery of the fiber

(Boyle et al., 2003) leads to excessive intracellular diffusion distances that constrain aerobic metabolic processes (Fig. 1). A requirement for comparing the effects of fiber size on recovery is that crabs from all size classes perform the same amount of chemical work during exercise. During burst contraction, intracellular AP stores are initially consumed to power contraction, after which anaerobic glycogenolysis is recruited to generate additional ATP for sustained bouts of locomotion (England and Baldwin 1983; Booth and McMahon, 1985; Head and Baldwin, 1986; Milligan et al., 1989; Morris and Adamczewska, 2002). The resting concentration of AP (and glycogen) and the activity of AK do not change with increasing body size in crustacean white muscle (Baldwin et al., 1999). Therefore, the contribution of AP to total ATP production during exercise is constant across all of the animal size classes used in the present study. It follows that lactate production alone is an effective indicator of potential differences among size classes in the amount of anaerobic work that occurred during exercise. The lack of significant differences among size classes in muscle lactate production during contraction (Fig. 5) indicates that muscle tissues from animals of all size classes incurred equal levels of mass-specific oxygen debt.

Boyle et al. (2003) described some of the metabolic impacts of increased fiber size in white levator muscle of blue crabs. They found that following burst exercise, glycogen depletion was greater and glycogen recovery was much slower in the larger animals than in small. These authors suggested that the extreme intracellular diffusion distances in the white fibers of large animals were responsible for the relatively slower rate of glycogen recovery. In addition, differences in diffusive flux rates in fibers of different sizes may be further amplified by the time dependent decrease in metabolite diffusion coefficients in muscle tissue, which results from intracellular barriers that obstruct net molecular motion across muscle fibers (Kinsey et al., 1999;

Kinsey and Moerland, 2002). Boyle et al. (2003) further argued that the greater glycogen depletion in larger animals occurred because white muscle fibers were relying more on anaerobic glycogenolysis to speed up certain phases of the post-contractile recovery cycle to more rapidly restore contractile function. This conclusion was based on the low ATP yield per glucosyl unit during anaerobic glycogenolysis, which results in greater glycogen depletion during recovery. The present study confirms the hypothesis posed by Boyle et al. (2003) by providing direct evidence that post-contractile anaerobic metabolism is size-dependent in white muscle fibers from blue crabs. Since a very large fraction of the post-contractile lactate production in white fibers diffuses into the blood, the differences among size classes in the anaerobic contribution to recovery are certain to be much more dramatic than is apparent from the muscle lactate data alone (Figs. 6, 7).

These arguments raise the question of which post-contractile recovery processes are likely to be accelerated by invoking anaerobic metabolism, and how would this benefit the animal? The most likely candidates are the recovery of AP and the restoration of ionic gradients across the membrane. Although not measured in the present study, there is evidence that AP recovery is relatively rapid (Ellington, 1983; Head and Baldwin, 1986; Thébault et al., 1987; Morris and Adamczewska, 2002) and is associated with post-contractile glycogen depletion and lactate accumulation in adult crustacean white muscle (England and Baldwin, 1983; Head and Baldwin, 1986; Kamp, 1989; Henry et al., 1994; Morris and Adamczewska, 2002; Boyle et al., 2003). Since AP is the fuel initially used during burst-activity (England and Baldwin, 1983; Head and Baldwin, 1986; Kamp, 1989; Baldwin et al. 1999), the rapid replenishment of AP across the entire cell would facilitate additional bouts of high-force anaerobic contractions. In contrast to crustaceans, vertebrates rely exclusively on aerobic metabolism to power resynthesis

of the phosphagen, phosphocreatine (PCr), and lactate does not accumulate following contraction (Kushmerick, 1983; Meyer, 1988; Curtin et al., 1997). The vertebrate pattern of recovery therefore appears to closely resemble that in white and dark levator muscle fibers from the small and medium animal size classes in this study (Fig. 6A), which entails a rapid, aerobic restoration of both phosphagen and lactate levels.

The relatively short intracellular diffusive distances in dark levator muscle fibers (Tse et al., 1983) (Fig. 2) led to the expectation that metabolic recovery following exercise would not lead to size dependent lactate production in this tissue. The observed differences in post-contractile lactate dynamics among the animal size classes were, therefore, not expected, however, these differences were less dramatic than in white fibers, which is consistent with my hypotheses (Fig. 6, 7). It is possible that dark fibers also produce lactate following contraction in an effort to speed up recovery, although it would be difficult to make the argument that this is due to intracellular diffusion constraints. In this view, the size dependence would simply reflect the mass-specific decrease in aerobic capacity that typically accompanies increases in body mass (Fig. 4), and anaerobic metabolism is used to preserve a rapid post-contractile recovery rate as animals grow larger. This interpretation may imply that, at the very least, diffusion constraints are embodied in the differences in the size dependence of lactate production between dark and white muscles seen in Figures 6 and 7. However, it could also be argued that the relatively low SA:V of the white fibers leads to slower lactate efflux and hence elevated post-contractile lactate accumulation that does not result from production rates that are greater than in dark fibers.

While the explanations above suggest some effects of diffusion on metabolic flux, I believe that the differences between dark and white fibers are actually much greater than is apparent in Figure 6. There are two likely explanations for artificially large differences among

size classes in dark fibers. First, following exercise, the circulating hemolymph is highly concentrated with lactate for an extended period of time. The bulk of the lactate that is released to the hemolymph during, and particularly after contraction is expected to arise from the white fibers (Fig. 6). The lactate-laden hemolymph also perfuses the dark levator muscle, however, and there is likely to be net diffusive flux of lactate from the hemolymph into the dark fibers. Second, the fiber composition of the dark levator muscle is heterogeneous, and the small, aerobic fibers located in the core are surrounded by giant white fibers (Tse et al., 1983). If the white fibers are producing most of the lactate after contraction, the close proximity of the dark fibers to the surrounding white fibers are likely to also allow for net lactate diffusion into the dark fibers. Therefore, the present whole animal experiments may not be adequate to fully resolve differences in the fiber size dependence of lactate dynamics between white and dark muscle. An analysis of isolated fibers would be a useful approach to address this issue.

Another argument for the presence of diffusive limitations in these large white fibers can be made by examining the scaling of the activity of the aerobic enzyme, citrate synthase (Fig. 5). The body mass scaling exponent of CS activity for dark muscle was more negative (b = -0.19) than for the white muscle (b = -0.09), meaning that there were greater differences among animal size classes in dark muscle than in white (Boyle et al., 2003). This result leads to the expectation that there would be greater differences in post-exercise lactate dynamics among size classes in the dark muscle than in the white muscle, which is contrary to both my predictions and observations.

In summary, although dark levator aerobic fibers of *C. sapidus* grow hypertrophically, reaching very large sizes similar to white levator muscle fibers, the fibers become increasingly subdivided throughout development and maintain a mean subdivision diameter of ~35 μm. This

developmental pattern leads to a constant size for each metabolic functional unit, while each contractile functional unit increase in size as the animal grows. Mitochondria occupy ~25 % of the volume of dark levator aerobic fiber subdivisions in all size classes of animals, although this morphological observation is in contrast to the negative scaling of mass-specific CS activity. The time course of lactate removal from tissues following exercise were consistent with the prediction that post-contractile metabolic recovery is size dependent in white locomotor muscle fibers of *C. sapidus*. Large white fibers appear to rely on anaerobic metabolism to accelerate certain phases of the metabolic recovery process to offset apparent diffusive limitations that may make aerobic metabolism unacceptably slow. Although the aerobic dark locomotor fibers, which should not be diffusion limited, also demonstrated size dependence of anaerobic recovery, this result may be due to an inability to fully resolve differences between muscle tissue types in a whole-animal experiment.

Figure 1. Arginine kinase (AK) mediates ATP-equivalent flux in crustacean muscle. Diffusive flux of arginine phosphate (AP) occurs over short distances in small white fibers of juvenile crabs (top), but as the fibers grow, diffusive flux must occur across hundreds of microns (bottom). Consequently, there is expected to be a reduction in rates of aerobic processes, such as aerobic recovery following exercise, as fiber size increases during development. In large fibers of adult crustaceans anaerobic glycogenolysis occurs following contraction presumably to speed up phases of the recovery process.

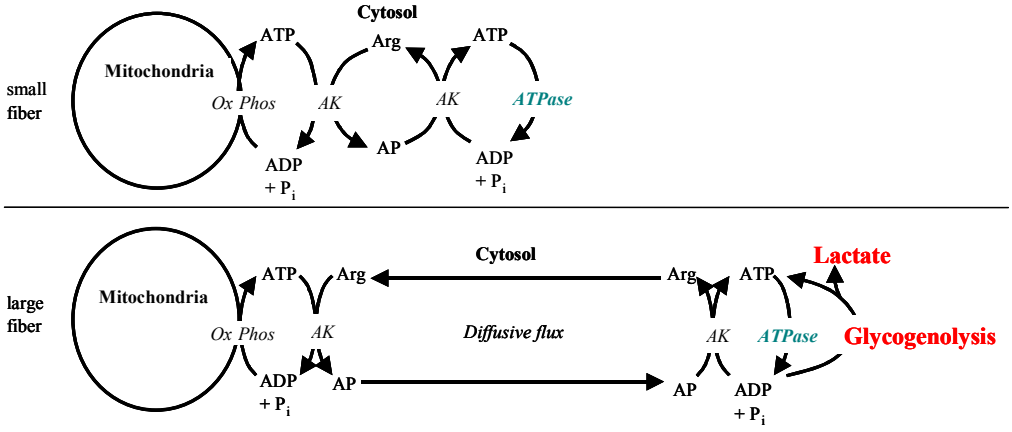
small
fiber
Mitochondria
Ox Phos
AK
Cytosol
Arg
ATP
ATP
AK
ATPase
AP
ADP
+ Pi
ADP
+ Pi
large
fiber
Mitochondria
Ox Phos
AK
ATP
Arg
Cytosol
Arg
ATP
Lactate
Diffusive flux
AK
ATPase
Glycogenolysis
ADP
+ Pi
AP
AP
ADP
+ Pi

Figure 2. Dark levator muscle fiber subdivision development. TEM of fiber subdivisions from (A) very small (B) small (C) medium and (D) large crabs are shown in the left panels. The middle panels show highlighted mitochondria from the subdivisions, and the panels on the right show highlighted subdivisions found in the micrographs in the left panels.

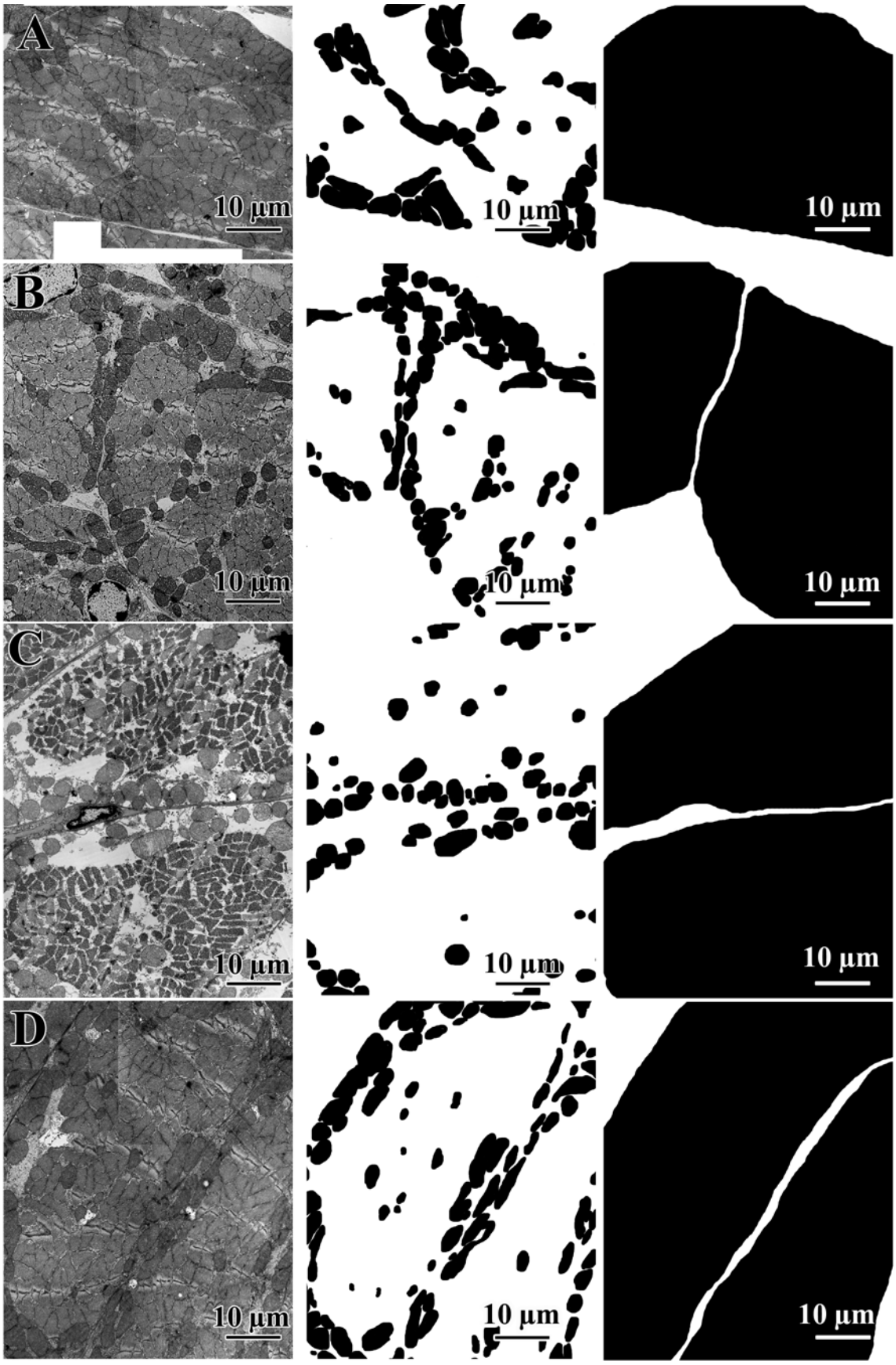
A
10 μm
10 μm
10 μm
B
10 μm
10 μm
10 μm
C
10 μm
10 μm
10 μm
D
10 μm
10 μm
10 μm

Figure 3. Mean mitochondrial fractional areas (open bars, left axis) and mean fiber subdivision diameters (filled bars, right axis) of the dark levator aerobic muscle fibers with respect to animal size class. Mitochondrial fractional area represents between 20-30% of the total area of each subdivision and does not scale with increasing body mass. Mean fiber subdivisions remain between 20 and 60 μm consistently throughout development.

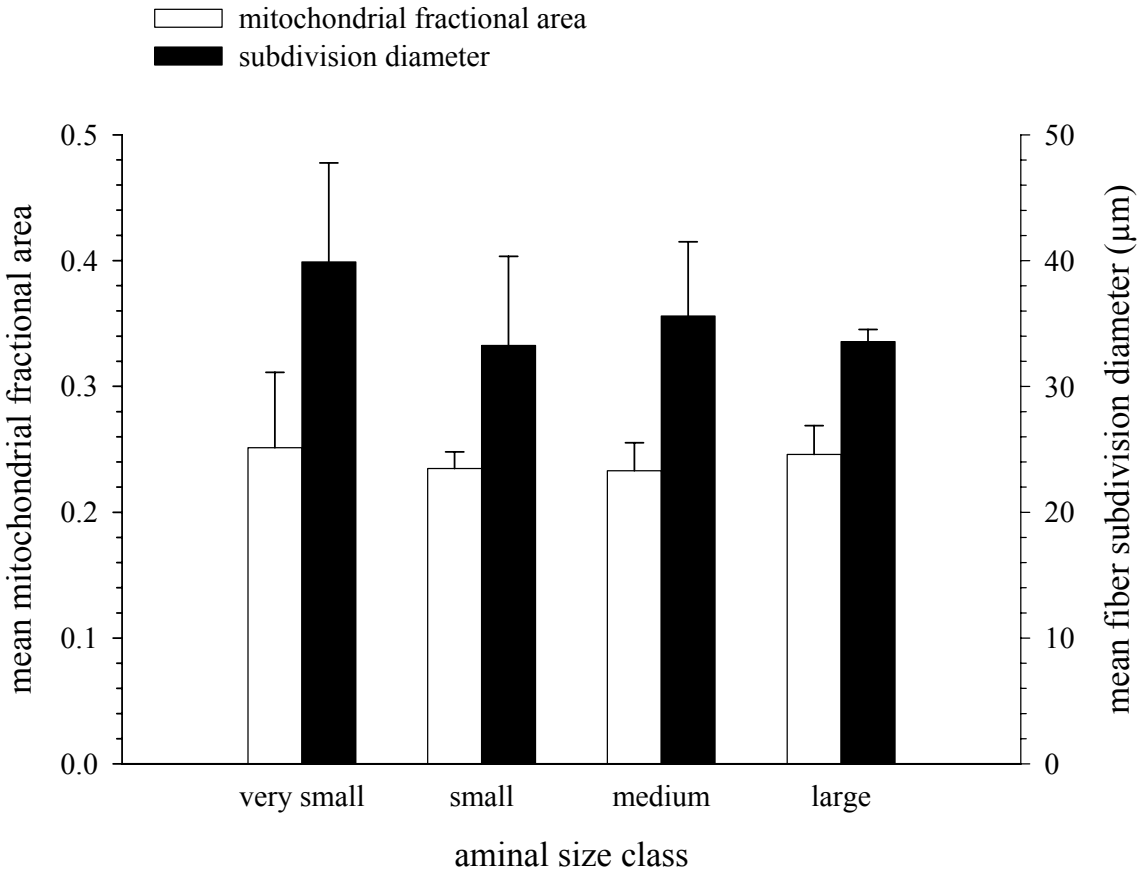
mitochondrial fractional area
subdivision diameter
mean mitochondrial fractional area
mean fiber subdivision diameter (µm)
0.0
0.1
0.2
0.3
0.4
0.5
0
10
20
30
40
50
very small
small
medium
large
aminal size class

Figure 4. Mass-specific scaling of citrate synthase (CS) activity per gram of white levator (open circles, data from Boyle *et al*. 2003) and dark levator muscle (filled circles). (A) The linear regression fit to the data is the log of the scaling equation CS activity = $(25.75)\cdot M^{-0.19}$ (R^2= 0.45) and in white levator muscle CS activity=$(5.0)\cdot M^{-0.09}$ (R^2=0.39) (B) Mean CS activity grouped by size class. Note the greater fractional differences between size classes in the dark levator muscle, than the white levator muscle. An * indicates that CS activity for that group is significantly different from the other two groups

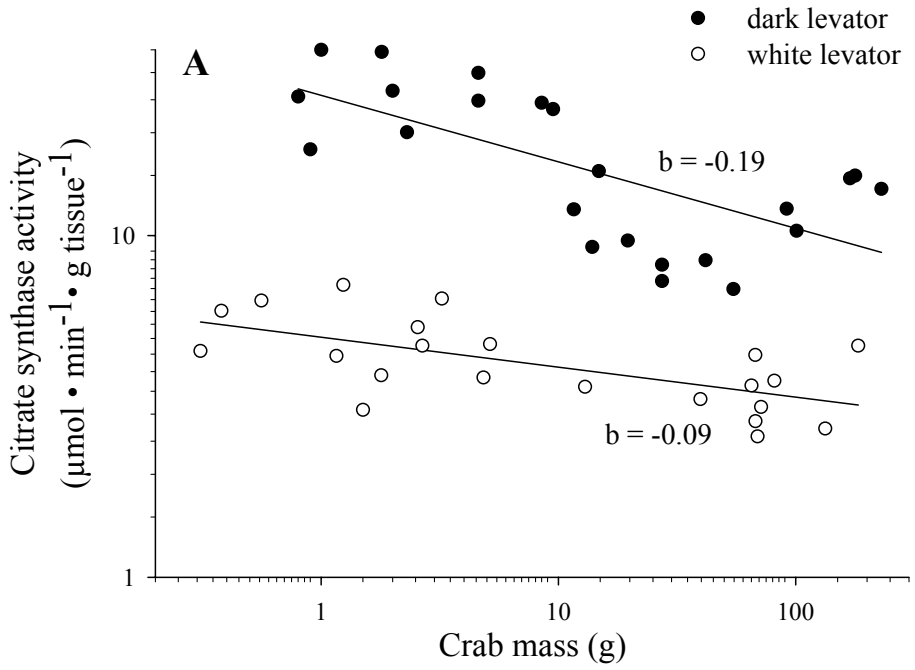
A
dark levator
white levator
b = -0.19
b = -0.09
Citrate synthase activity
(µmol • min-1 • g tissue-1)
10
1
1
10
100
Crab mass (g)

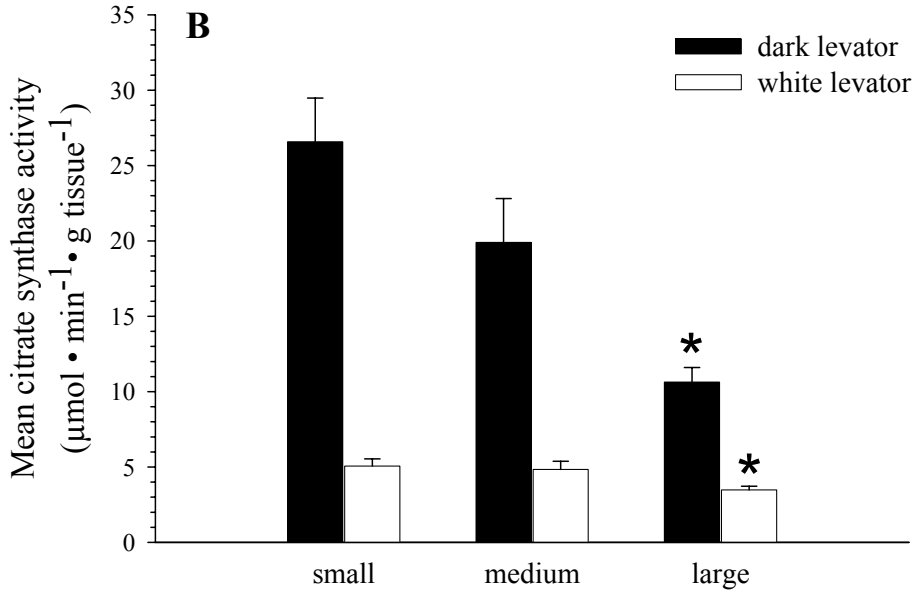
B
dark levator
white levator
Mean citrate synthase activity
(µmol • min-1 • g tissue-1)
35
30
25
20
15
10
5
0
*
*
small
medium
large

Figure 5. Lactate (mM) concentrations at rest, 1 min after exercise, and 60 min after exercise in (A) white levator and (B) dark levator muscles. Note in (A) and (B) that resting and 1 min values are similar among the size classes. At 60 min, lactate begins to decrease in both tissues from small and medium crabs, while it remains elevated in large dark and white levator muscles. An * indicates that lactate concentrations for that group were significantly different from the other two groups.

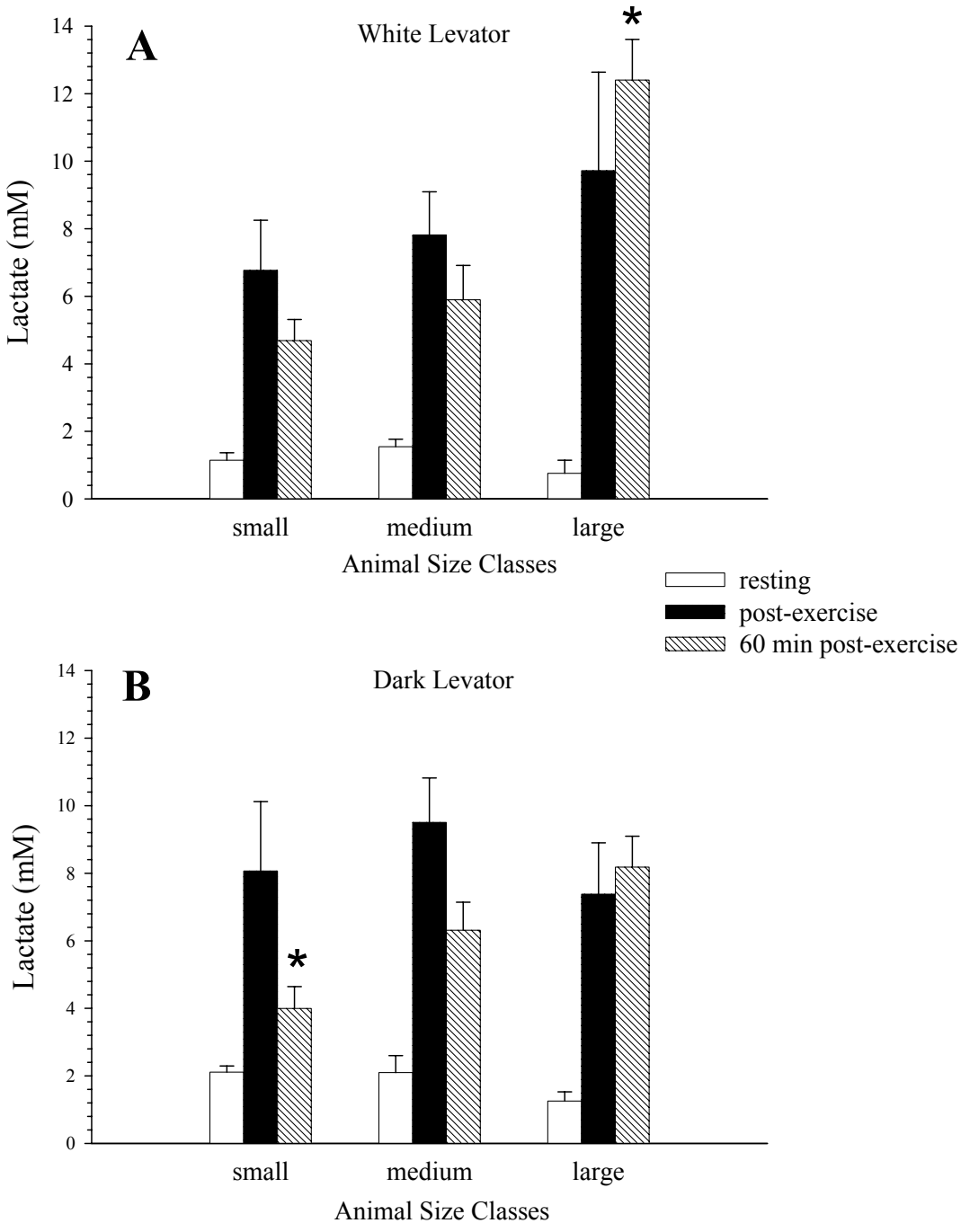
A
White Levator
*
Lactate (mM)
14
12
10
8
6
4
2
0
small
medium
large
Animal Size Classes
resting
post-exercise
60 min post-exercise
B
Dark Levator
*
Lactate (mM)
14
12
10
8
6
4
2
0
small
medium
large
Animal Size Classes

Figure 6. Time course of lactate concentration changes in (A) white and (B) dark levator muscles, and (C) hemolymph following fatiguing exercise. Resting values are plotted first. The 0 min time point starts immediately following exercise. Note the continuing increase in lactate following exercise in (A) white fibers from large crabs, and the prolonged period of time for lactate removal from all tissues in large crabs. The differences among the size classes appear to be less in the dark levator muscle (B).

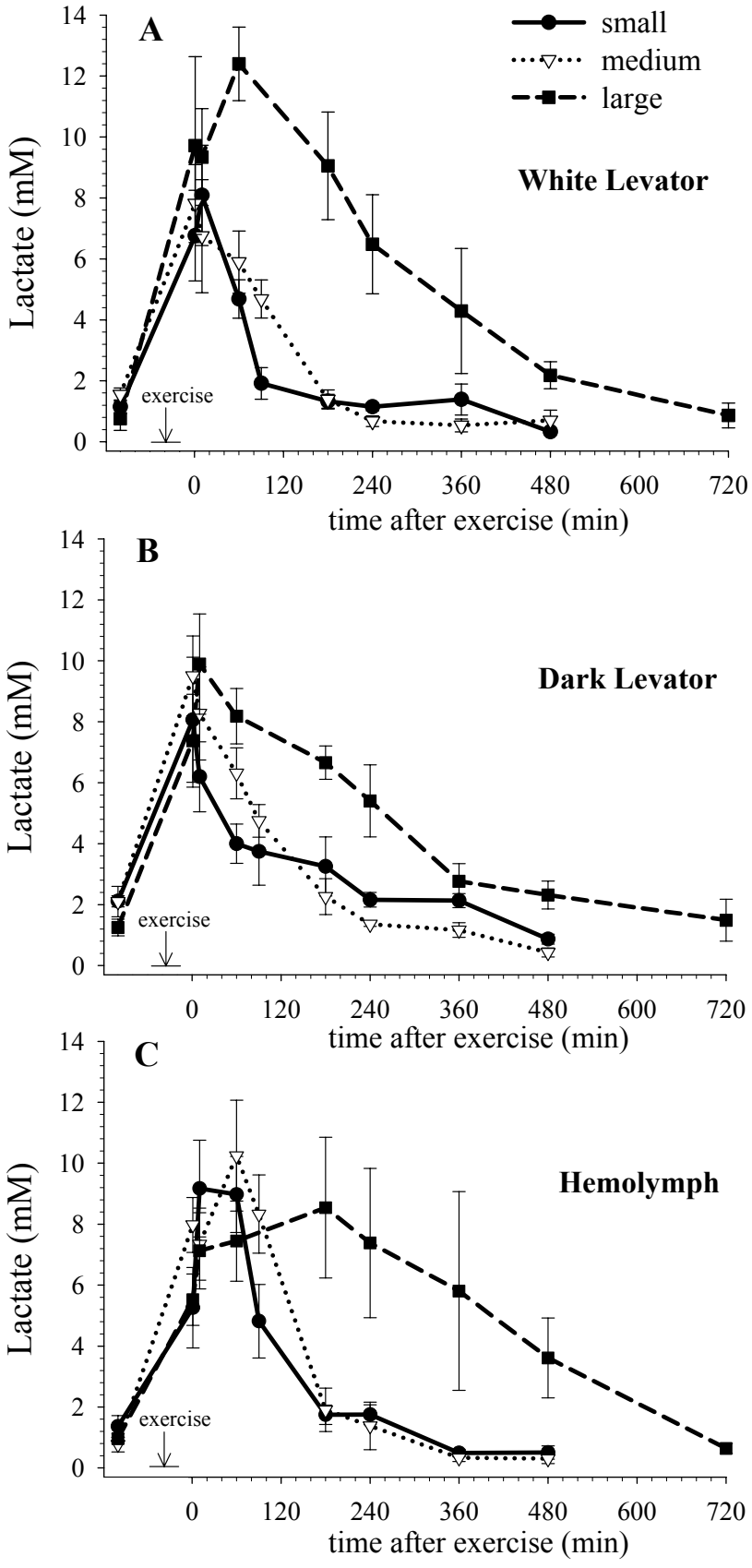
A
small
medium
large
White Levator
Lactate (mM)
exercise
time after exercise (min)
B
Dark Levator
Lactate (mM)
exercise
time after exercise (min)
C
Hemolymph
Lactate (mM)
exercise
time after exercise (min)

Figure 7. The area under the lactate concentration recovery curve for each tissue vs. size class. The post recovery lactate concentration curves in Fig. 6 were integrated beginning at the 10 min time point. Note the differences between the white and dark levator muscles in large crabs.

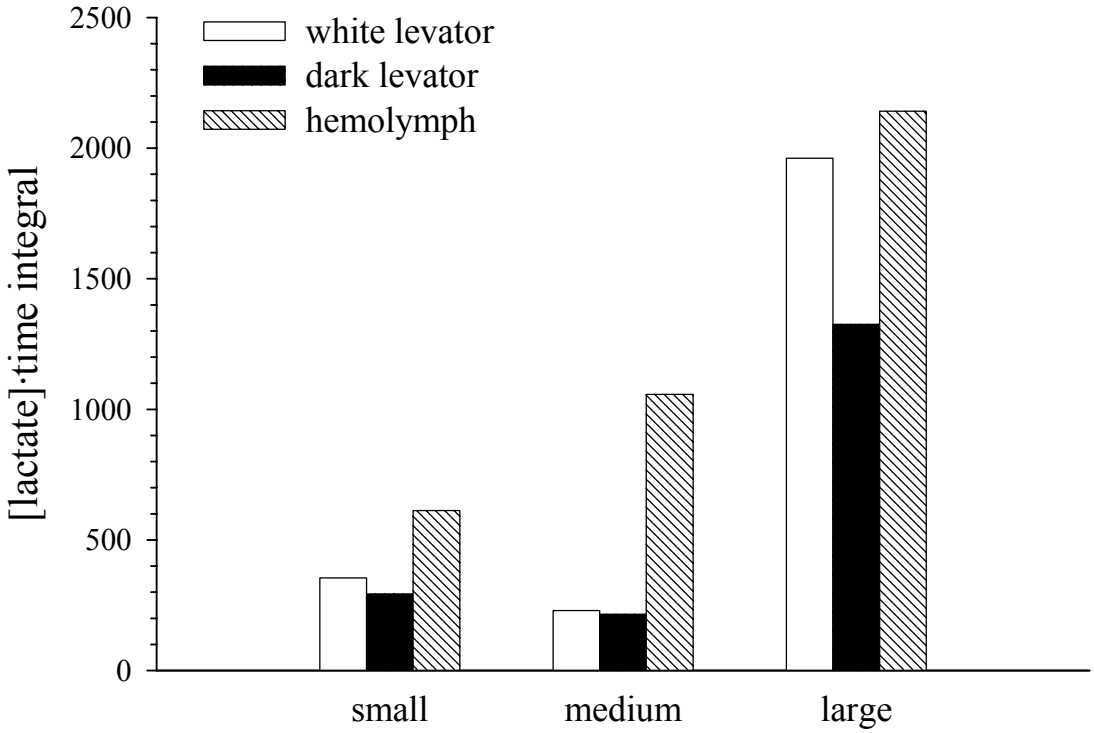
white levator
dark levator
hemolymph
[lactate]·time integral
2500
2000
1500
1000
500
0
small
medium
large

TEM			CS activity			Lactate production and removal		
SIZE CLASS	**MEAN WEIGHT (g)**	**WEIGHT RANGE (g)**	**SIZE CLASS**	**MEAN WEIGHT (g)**	**WEIGHT RANGE (g)**	**SIZE CLASS**	**MEAN WEIGHT (g)**	**WEIGHT RANGE (g)**
Very Small (N = 3)	0.119 ± 0.0131	0.0957-0.1411						
Small (N = 3)	1.12 ± 0.128	0.90-1.34	Small (N = 6)	1.47 ± 0.26	0.8-2.3	Small (N = 58)	1.29 ± 0.06	0.4-2.3
Medium (N = 3)	11.0 ± 3.38	5.2-16.9	Medium (N = 7)	9.64 ± 1.55	4.6-14.8	Medium (N = 49)	13.25 ± 3.9	3.7-23.1
Large (N = 3)	181.6 ± 6.13	171.1-192.5	Large (N = 10)	94.0 ± 23.6	27.3-229.7	Large (N = 51)	227.7 ± 6.86	130.6-310.4

Table 1. Size classes of crabs used in this study based on body mass and white levator fiber diameter data from Boyle et al. (2003) and dark fiber subdivision data derived from TEM analysis. All numbers area represented as mean ± sem.

REFERENCES

Baldwin, J., Gupta, A. and Iglesias, X. (1999). Scaling of anaerobic energy metabolism during tail flipping behaviour in the freshwater crayfish, C*herax destructor*. *Mar. Freshwater Res.* **50**,183-187.

Bittner, G.D. and Traut, D.L. (1978). Growth of crustacean muscles and muscle fibers. *J. Comp. Physiol.* **124**, 277-285.

Booth, C.E. and McMahon, B.R. (1985). Lactate dynamics during locomotor activity in the blue crab, *Callinectes sapidus*. *J. Exp. Biol.* **118**, 461-465.

Booth, C.E and McMahon, B.R. (1992). Aerobic capacity of the blue crab, *Callinectes sapidus*. *Physiol. Zool.*. **65**, 1074-1091.

Boyle, K.L., Dillaman, R.M. and Kinsey, S.T. (2003). Mitochondrial distribution and glycogen dynamics suggest diffusion constraints in muscle fibers of the blue crab, *Callinectes sapidus*. *J. Exp. Zool.* **297A**, 1-16.

Carpenè, E. and Veggetti, A. (1981). Increase in muscle fibres in the lateralis muscle (white portion) of Mugilidae (Pisces, Teleostei). *Experientia*. **37**, 191-193.

Cochran, D.M. (1935). The skeletal musculature of the blue crab, *Callinectes sapidus Rathbun*. *Smithsonian Misc. Collec.* **92**(No. 9), 1-76.

Curtin, N.A., Kushmerick, M.J., Wiseman, R.W. and Woledge, R.C. (1997). Recovery after contraction of white muscle fibres from the dogfish, *Scyliorhinus canicula*. *J. Exp. Biol.* **200**, 1061-1071.

Egginton, S. and Sidell, B.D. (1984). Thermal acclimation induces adaptive changes in subcellular structure of fish skeletal muscle. *Am. J. Physiol.* **25**, R1-R9.

Ellington, W.R. (1983). The recovery from anaerobic metabolism in invertebrates. *J. Exp. Zool.* **228**, 431-444.

Ellington, W.R. (2001). Evolution and physiological roles of phosphagen systems. *Ann. Rev. Physiol.* **63**, 289-325.

Ellington, W.R. and Kinsey, S.T. (1998). Functional and evolutionary implications of the distribution of phosphagens in primitive-type spermatazoa. *Biol. Bull.* **195**, 264-272.

England, W.R. and Baldwin, J. (1983). Anaerobic energy metabolism in the tail musculature of the Australian yabby, *Cherax destructor*: role of phosphagens and anaerobic glycolysis during escape behavior. *Physiol. Zool.* **56**, 614-622.

Head, G. and Baldwin, J. (1986). Energy metabolism and the fate of lactate during recovery

from exercise in the Australian freshwater crayfish, *Cherax destructor*." *Aust. J. Mar. Freshw. Res.* **37**, 641-646.

Henry, R.P., Booth, C.E., Lallier, F.H. and Walsh, P.J. (1994). Post-exercise lactate production and metabolism in three species of aquatic and terrestrial decapod crustaceans. *J. Exp. Biol.* **186**, 215-234.

Holt, S.M. and Kinsey, S.T. (2002). Osmotic effects on arginine kinase flux in muscle from the blue crab, *Callinectes sapidus*. *J. Exp. Biol.* **205**, 1775-1785.

Howard, C.V. and Reed, M.G. (1998). Unbiased stereology, 3-dimensional measurements in microscopy. Oxford: BIOS Scientific Publishers.

Jahromi, SS and Atwood, HL. (1971). Structural and contractile properties of lobster leg-muscle fibers. *J. Exp. Zool.* **176**, 475-486.

Johnston, I.A., Fernández, D.A., Calvo, J., Vieira, V.L.A., North, A.W., Abercromby, M. and Garland, T. Jr. (2003). Reduction in muscle fibre number during the adaptive radiation of notothenioid fishes: a phylogenetic perspective. *J. Exp. Biol.* **206**, 2595-2609.

Judy, M.H. and Dudley, D.L. (1970). Movements of tagged blue crabs in North Carolina waters. *Comm. Fish. Rev.* **32**, 29-35.

Kamp, G. (1989). Glycogenolysis during recovery from muscular work. *Biol. Chem. Hoppe-Swyler.* **370**, 565-573.

Kim, S.K., Yu, S.H., Jeong-Hwa, S., Hübner, H. and Buchholz, R. (1998). Calculations on O_2 transfer in capsules with animal cells for the determination of maximum capsule size without O_2 limitation. *Biotech. Letters*. **20**, 549-552.

Kinsey, S.T., Penke, B., Locke, B.R. and Moerland, T.S. (1999). Diffusional anisotropy is induced by subcellular barriers in skeletal muscle. *NMR in Biomedicine.* **11**, 1-7.

Kinsey, S.T. and Moerland, T.S. (2002). Metabolite diffusion in giant muscle fibers of the spiny lobster, *Panulirus argus*. J. Exp. Biol. **205**, 3377-3386.

Kushmerick, M. (1983). Energetics of muscle contraction. In: *Handbook of Muscle Physiology-Skeletal Muscle*. (ed. L.D. Peachy, R.H. Adrian and S.R. Geiger), pp. 189-236. Bethesda: Amer. Physiol. Society.

Lowry, O. H. and Passonneau, J.V. (1972). Lactate: Method II. In: *A Flexible System of Enzymatic Analysis*. pp. 199-201. New York, London: Academic Press.

Meyer, R.A., Sweeney, H.L. and Kushmerick, M.J. (1984). A simple analysis of the 'phosphocreatine shuttle.' *Am. J. Physiol.* **246**, C365-377.

Meyer, R.A. (1988). A linear model of muscle respiration explains monoexponential phosphocreatine changes. *Am. J. Physiol.* **254**, C548-C553.

Mainwood, G.W. and Raukusan, K. (1982). A model for intracellular energy transport. *Can. J. Physiol. Pharmacol.* **60**, 98-102.

Milligan C.L., Walsh P.J., Booth C.E. and McDonald D.L. (1989). Intracellular acid-base regulation during recovery from locomotor activity in the blue crab, *Callinectes sapidus*. *Physiol. Zool.* **62,** 621-638.

Morris, S. and Adamczewska, A.M. (2002). Utilisation of glycogen, ATP, and arginine phosphate in exercise and recovery in terrestrial red crabs, *Gecarcoidea natalis*. *Comp. Biochem. Physiol. A*. **133**, 813-825.

Pecl, G.T. and Moltschaniwskyj, N.A. (1997). Changes in muscle structure associated with somatic growth in *Idiosepius pygmaeus*, a small tropical cephalopod. *Zool. Lond.* **242**, 751-764.

Preshnell, J.K. and Schriebman, M.P. (1997). Humason's animal tissue techniques. Baltimore: Johns Hopkins University Press.

Preuss, T., Lebaric, Z.N. and Gilly, W.F. (1997). Post-hatching development of circular mantle muscles in the squid, *Loligo opalescens*. *Biol. Bull.* **192**, 375-387.

Reynolds, E.S. (1963). The use of lead citrate at high pH as an electron opaque stain in electron microscopy. *J. Cell Biol.* **17**, 208-212.

Roer, R. and Dillaman, R. (1984). The structure and calcification of the crustacean cuticle. *Amer. Zool.* **24**, 893-909.

Rome, L.C. and Lindstedt, SL. (1998). The quest for speed: muscles built for high-frequency contractions. *NIPS*. **13**, 261-268.

Rosenbluth, J. (1969). Sarcoplasmic reticulum of an unusually fast-acting crustacean muscle. *J. Comp. Biol.* **42**, 534-547.

Rowlerson, A. and Veggetti, A. (2001). Cellular mechanisms of post-embryonic muscle growth in aquaculture species. In: *Muscle development and growth*. (ed. I. Johnston), pp. 103-140. San Diego: Academic Press.

Russel, B., Motlagh, D. and Ashley, W.W. (2000). Form follows function: how muscle shape is regulated by work. *J. Appl. Physiol.* **88**, 1127-1132.

Schmidt-Nielsen, K. (1984). Problems of size and scale. In: *Scaling: why is animal size so important?* p. 15. Cambridge: Cambridge University Press.

Spurr, R.A. (1969). A low-viscosity epoxy resin embedding medium for electron microscopy. *J.*

Ultrastruct. Res. **26**, 31-43.

Thébault, M.T., Raffin, J.P. and LeGall, J.Y. (1987). In vivo ^{31}P NMR in crustacean muscles: fatigue and recovery in the tail musculature from the prawn, *Palaemon elegans. Biochem. Biophys. Res. Comm.* **145**, 453-459.

Tse, F.W., Govind, C.K. and Atwood, H.L. (1983). Diverse fiber composition of swimming muscles in the blue crab, *Callinectes sapidus*. *Can. J. Zool.* **61**, 52-59.

Walsh, PJ and Henry, RP. (1990). Activities of metabolic enzymes in the deep-water crabs *Caceon fenneri* and *C. quinquedens* and the shallow-water crab *Callinectes sapidus*. *Mar. Biol.* **106**, 343-346.

White, AQ and Spirito, CP. (1973). Anatomy and physiology of the swimming leg musculature in the blue crab, *Callinectes sapidus*. *Mar. Behav. Physiol.* **2**, 141-153.

Weatherly, A.H. and Gill, H.S. (1985). Dynamics of increase in muscle fibers in teleosts in relation to size and growth. *Experientia.* **41**, 353-354.

Weatherly, A.H. and Gill, H.S. (1987). Chapter 5: Tissues and Growth. In: *The Biology of Fish Growth*, pp. 147-175. London: Academic Press.

Willemse, J.J. and Lieuwma-Noordanus, C. (1984). The generation of 'new' white muscle fibres by budding in the lateral musculature of elvers, *Anguilla anguilla* (L.) during normal development. *Experientia*. **40**, 990-992.